$\mathcal{P}, \mathcal{T}$-odd Faraday rotation in heavy neutral atoms

D. V. Chubukov,[1,2] L. V. Skripnikov,[2,1] and L. N. Labzowsky[1,2]
[1]*St. Petersburg State University, Ulyanovskaya 3, St. Petersburg 198504, Petrodvorets, Russia*
[2]*Petersburg Nuclear Physics Institute named by B.P. Konstantinov of National Research Centre "Kurchatov Institut," St. Petersburg 188300, Gatchina, Russia*

(Received 2 April 2018; published 28 June 2018)

Accurate evaluation of the $\mathcal{P},\mathcal{T}$-odd Faraday effect (rotation of the polarization plane of the light propagating through a medium in the presence of an external electric field) is presented. The magnitude of this rotation is directly proportional to the optical path length. A novel idea is to observe the $\mathcal{P},\mathcal{T}$-odd Faraday effect using intracavity absorption spectroscopy (ICAS) experiments. The modern ICAS experiments allow one to observe the rotation of the light polarization plane (natural or $\mathcal{P}$-odd) with the optical path length up to a hundred kilometers. This can be done mainly due to the work off-line in the resonance absorption experiments. For the Faraday rotation (ordinary or $\mathcal{P},\mathcal{T}$-odd) the maximum of the effect coincides with the maximum of absorption which usually prevents the work off-line and employment of the large optical path length. However, we propose to use the second rotation maximum that exists for the Faraday effect and would also allow for work off-line. The calculations are performed for the heavy metal atoms Cs, Tl, Pb, and Ra where the $\mathcal{P},\mathcal{T}$-odd effects are most pronounced. The results of the calculations demonstrate that with the large optical path length the ICAS experiments will be able to fix the possible $\mathcal{P},\mathcal{T}$-odd effects at a level comparable with other very advanced modern experiments.

DOI: 10.1103/PhysRevA.97.062512

I. INTRODUCTION

The existence of the $\mathcal{T}$-noninvariant (time-noninvariant) interactions in nature is one of the most important fundamental problems which has to be solved by modern physics. The $\mathcal{CP}$ violation ($\mathcal{C}$ - charge conjugation, $\mathcal{P}$ - space inversion) discovered in [1] in exotic reactions with K mesons means, according to the $\mathcal{CPT}$ theorem, that such interactions in principle exist. However, the search for more universal $\mathcal{T}$-violating interactions has been continued from 1950 up to now without success. The existence of the electric dipole moment (EDM) for any particle (not truly neutral, i.e., not coinciding with itself after charge conjugation), i.e., for electron, nucleon, charged boson, etc., would mean both $\mathcal{P}$ and $\mathcal{T}$ violation. The same concerns any closed system of such particles: atom, molecule, nucleus. The first suggestion for the search for the EDM was made in [2] for neutrons in 1950 and for electrons in atoms in 1958 [3]. Later it was found that in heavy atoms the electron EDM can be strongly enhanced compared to the EDM of free electrons [4,5]. Even stronger enhancement for the nuclear EDM in heavy diatomic molecules was predicted in [6], where molecules with closed electron shells were considered. In [7,8] it was found that very strong enhancement (up to 1 billion times) can arise in heavy diatomic molecules with open electron shells for $\mathcal{P}$-odd effects due to the existence of the Λ-doubling effect, which is absent for closed-shell molecules. In [9] the same enhancement in diatomic molecules was predicted for the electron EDM and in [10] for the $\mathcal{P},\mathcal{T}$-odd interaction between the electron and the nucleus. In [10] it was also demonstrated that the $\mathcal{P},\mathcal{T}$-odd electron-nucleus interaction effect cannot be distinguished from the electron EDM effect in any experiment with any particular atom or molecule. According to [11] this can be done in the series of experiments with highly charged ions due to the different dependence of the two effects on the nuclear charge Z. The most restrictive bounds for the electron EDM were established in experiments with Tl atoms ($d_e < 1.6\times10^{-27}\ e\,\mathrm{cm}$) [12], YbF molecules ($d_e < 1.05\times10^{-27}\ e\,\mathrm{cm}$) [13], ThO molecules ($d_e < 0.87\times10^{-28}\ e\,\mathrm{cm}$) [14], and HfF^+ molecular ions ($d_e < 1.3\times10^{-28}\ e\,\mathrm{cm}$) [15]. For extraction of d_e values from the experimental data the theoretical calculations of the enhancement coefficient are necessary. These calculations become especially sophisticated for molecules (see, e.g., [16–18]).

Concerning the theoretical predictions for the value d_e within the standard model (SM), the situation remains rather uncertain. It was early understood that the $\mathcal{CP}$-violating effects within the SM can arise only via the phase factor in the Cabibbo-Kobayashi-Maskawa (CKM) matrix. In particular, the electron EDM can arise if the three-loop vertex is introduced, including one quark loop which provides the CKM phase [19]. In [19] the loop integrals were calculated numerically with the Glashow-Iliopoulos-Maiani (GIM) mechanism taken into account. The value obtained in [19] for the electron EDM was $d_e \approx 10^{-38}\ e\,\mathrm{cm}$. However, later in [20] it was demonstrated that the total result at the three-loop level should be exactly zero due to cancellations between different terms. In [20] it was suggested that with additional gluon exchange (i.e., already at the four-loop level) the result will become nonzero. In [21] a particular mechanism of the $\mathcal{P},\mathcal{T}$-odd electron-nucleus interaction via two-photon exchange with one $\mathcal{CP}$-violating vertex on the electron line was suggested. The estimates for this mechanism, which the authors called "benchmark," gave the value $d_e^{\mathrm{eqv},2\gamma} \approx 10^{-38}\ e\,\mathrm{cm}$ for the "equivalent" electron EDM. This "equivalent" EDM can be

defined as an electron EDM that provides the same linear Stark shift in an atomic system as a given $\mathcal{P},\mathcal{T}$-odd electron-nucleus interaction in the same external electric field. In the same paper the "ordinary" electron EDM effect was estimated as $d_e \approx 10^{-44}\ e$ cm. This estimate was given exclusively on the basis of GIM, without numerical calculations. The contribution of the gluon exchange was expressed via the factor $\alpha_s/4\pi \approx 1/10$, where α_s is the strong interaction constant. From the other side, one can suppose that the cancellation found in [20] does not change the values of the separate terms evaluated in [19]. Then multiplying the value $10^{-38}\ e$ cm [19] by this factor we would obtain $d_e \approx 10^{-39}\ e$ cm. Recently in [22] another mechanism of the $\mathcal{P},\mathcal{T}$-odd electron-nucleus interaction in atomic systems was suggested, namely, an exchange by the Higgs boson between electron and nucleus with $\mathcal{CP}$-violating vertex on the electron line. This effect, unlike the electron EDM contribution, does not vanish in the three-loop approximation. Actually, the $\mathcal{P},\mathcal{T}$-odd electron-nucleus interaction in atomic systems was first introduced as an exchange by heavy neutral scalar particle [10]. The estimate for this effect correlates with the estimate for d_e and therefore ranges from $d_e^{\rm eqv} \approx 10^{-40}\ e$ cm to $d_e^{\rm eqv} \approx 10^{-45}\ e$ cm.

The $\mathcal{P},\mathcal{T}$-odd Faraday effect consists of rotation of the polarization plane for the light propagating through a medium in the presence of an external electric field oriented along the light propagation direction. This effect is fully similar to the ordinary Faraday effect which takes place in an external magnetic field. Unlike the ordinary Faraday effect, the $\mathcal{P},\mathcal{T}$-odd Faraday effect occurs only by violation of $\mathcal{P}$- and $\mathcal{T}$-reversal symmetries. The existence of such an effect was first predicted in [23], also mentioned in [9], and later discussed in [24]. If the frequency of propagating light is adjusted to an atomic (molecular) resonance the rotation angle for the light polarization plane is inversely proportional to the resonance linewidth Γ, both in the ordinary and $\mathcal{P},\mathcal{T}$-odd Faraday effects. The idea in [24] was to employ nonlinear optical effects to reduce the Γ value and consequently enhance the optical rotation angle. Experiments of this kind have been carried out since 2001 [25] (see also [26]). In these experiments a gas vapor cell with atomic Cs vapor was employed. However, as far as we know, the results have not yet been reported. In the present paper we revisit the $\mathcal{P},\mathcal{T}$-odd Faraday effect in view of significant progress in the intracavity absorption spectroscopy (ICAS) made during the last few decades [27–29]. We suggest to observe the $\mathcal{P},\mathcal{T}$-odd Faraday rotation off-resonance using a second Faraday rotation maximum existing both for the ordinary and $\mathcal{P},\mathcal{T}$-odd Faraday effects. This would allow one to employ very large optical path lengths pertinent in the recent ICAS experiments and greatly enhance the $\mathcal{P},\mathcal{T}$-odd Faraday rotation angle. Preliminary estimates on the subject were given recently in [30]. Here we present accurate calculations and a detailed analysis of the possible ICAS-type experiment.

Our paper is organized as follows. In Sec. II we describe how the $\mathcal{P},\mathcal{T}$-odd Faraday effect arises in atomic systems in the presence of the external electric field. We start from the expression for the optical rotation angle caused by arbitrary birefringence, describe how the birefringence arises in terms of quantum electrodynamics (i.e., how the light-scattering amplitude is connected with the refractive index), and discuss the linear Stark effect, which is the origin of the birefringence generating the $\mathcal{P},\mathcal{T}$-odd Faraday effect. In Sec. III we discuss in detail the theoretical grounds for the possible experiment: the magnitude of the optical rotation angle, absorption in an atomic vapor, and the existence of the second maximum for the Faraday rotation angle as a function of the detuning. In Sec. IV we briefly describe the powerful numerical methods that were used for evaluation of the linear Stark effect in heavy metal atoms and in particular, for the evaluation of the electron EDM enhancement coefficients. In Sec. V the numerical results are given for Cs, Tl, Pb, and Ra atoms. Discussion of the results and conclusions are given in Sec. VI.

II. LINEAR STARK SHIFT IN ATOMIC SYSTEMS AS AN ORIGIN OF THE $\mathcal{P},\mathcal{T}$-ODD FARADAY EFFECT

A. Faraday rotation angle and the refractive index

The rotation angle ψ for the polarization plane of the light propagating through the optically active medium with any type of birefringence (natural or $\mathcal{P}$-odd optical activity, ordinary or $\mathcal{P},\mathcal{T}$-odd Faraday effect) is defined by the relation (see, for example, [31])

$$\psi = \pi \frac{l}{\lambda} \mathrm{Re}(n_+ - n_-), \tag{1}$$

where l is the optical path length, λ is the wavelength, and $n_{+(-)}$ are the refractive indices for the right (left) circularly polarized light. In general, the refractive index for any resonant process in an atomic system is connected with the dynamic polarizability of this system $\alpha(\omega)$:

$$n(\omega) \approx 1 + 2\pi\rho\alpha(\omega). \tag{2}$$

Here ρ is the atomic number density. The polarizability has the same dimension as the volume, so the second term in the right-hand side of Eq. (2) is dimensionless. The formula (2) is valid when this second term is small compared to unity.

B. QED theory of the resonance dynamic polarizability of an atomic system

Quantum electrodynamical (QED) theory of the resonant processes in atomic systems can be found, for example, in [32]. In this section we consider a resonant process as a photon scattering on a heavy neutral atom with one valence electron in its ground state $ns_{1/2}$. The frequency of incident photon is adjusted for the resonant excitation of the state $n'p_{1/2}$ so that the transition will be of E1 type. For such transitions the Faraday rotation effect (ordinary or $\mathcal{P},\mathcal{T}$-odd) will be the largest. This process is described by the Feynman graph, Fig. 1. For our purposes it is convenient to consider only the elastic photon scattering.

An expression for the transition amplitude, corresponding to Fig. 1, is as follows [32]:

$$A^{\rm E1}_{ns_{1/2}(n'p_{1/2})} = e^2 \langle ns_{1/2}|\boldsymbol{\alpha}\boldsymbol{\mathcal{A}}^{\boldsymbol{k}_i,\boldsymbol{e}_i}_{\rm E1}(\boldsymbol{r})e^{i\boldsymbol{k}_i\boldsymbol{r}}|n'p_{1/2}\rangle \times \frac{\langle n'p_{1/2}|\boldsymbol{\alpha}\boldsymbol{\mathcal{A}}^{\boldsymbol{k}_f,\boldsymbol{e}_f*}_{\rm E1}(\boldsymbol{r})e^{-i\boldsymbol{k}_f\boldsymbol{r}}|ns_{1/2}\rangle}{E_{n'p_{1/2}} - E_{ns_{1/2}} - \omega}, \tag{3}$$

where $\boldsymbol{k}_i$, $\boldsymbol{e}_i$ and $\boldsymbol{k}_f$, $\boldsymbol{e}_f$ are the wave vectors and polarizations for the initial (absorbed) and final (emitted) photons, respectively; ω is the photon frequency. In the case of elastic

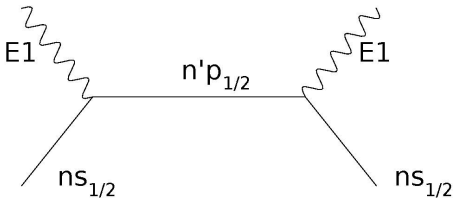

FIG. 1. The elastic resonant scattering of a photon on the ground $ns_{1/2}$ atomic state. The solid lines denote an atomic electron, and the wavy lines denote the absorbed and emitted photons. The time axis is supposed to be directed from left to right.

scattering, $\omega = |\boldsymbol{k}_i| = |\boldsymbol{k}_f|$. Dirac matrices are denoted as $\boldsymbol{\alpha}$, and $\boldsymbol{\mathcal{A}}^{\boldsymbol{k},\boldsymbol{e}}_{\rm E1}(\boldsymbol{r})$ is the E1 photon wave function in the coordinate space. Equation (3) is written in relativistic units (r.u.): $\hbar = c = m_e = 1$, where $\hbar$ is the Planck constant, c is the speed of the light, and m_e is the electron mass.

To introduce the line profile for the process depicted in Fig. 1 we have to sum up the infinite sequence of the lowest-order electron self-energy insertions into the internal electron line in Fig. 1 [32]. This leads to the arrival of the $n'p_{1/2}$ level width $\Gamma_{n'p_{1/2}}$ in the energy denominator in Eq. (3):

$$A^{\rm E1}_{ns_{1/2}(n'p_{1/2})} = e^2\langle ns_{1/2}|\boldsymbol{\alpha}\boldsymbol{\mathcal{A}}^{\boldsymbol{k}_i,\boldsymbol{e}_i}_{\rm E1}(\boldsymbol{r})e^{i\boldsymbol{k}_i\boldsymbol{r}}|n'p_{1/2}\rangle \times \frac{\langle n'p_{1/2}|\boldsymbol{\alpha}\boldsymbol{\mathcal{A}}^{\boldsymbol{k}_f,\boldsymbol{e}_f*}_{\rm E1}(\boldsymbol{r})e^{-i\boldsymbol{k}_f\boldsymbol{r}}|ns_{1/2}\rangle}{E_{n'p_{1/2}} - E_{ns_{1/2}} - \omega - \frac{i}{2}\Gamma_{n'p_{1/2}}}. \quad (4)$$

When describing the photon interaction with atomic electrons it is more convenient to characterize the photons with the set of quantum numbers ωjlm, where ω is the frequency, and jm are the angular momentum and its projection. The parity of the photon is determined by the value of l: the wave function of the magnetic-type photons (M) correspond to $l = j$ and the wave functions of the electric-type photons are the linear combinations of the states with $l = j \pm 1$. Then the parity of the magnetic-type photon is

$$P = (-1)^{j+1} \quad (5)$$

and the parity of the electric-type photon is

$$P = (-1)^{j}. \quad (6)$$

In this section we consider the polarizabilities, connected with the resonance scattering of electric (namely, dipole electric E1) photons. The polarizabilities connected with the absorption and emission of magnetic dipole (M1) photons were considered in connection with the $\mathcal{P}$-odd activity in atoms [33,34].

The explicit expressions for $\boldsymbol{\mathcal{A}}^{\rm (E)}_{\omega jm}(\boldsymbol{r})$ photon wave functions are [35]

$$\boldsymbol{\mathcal{A}}^{\rm (E)}_{\omega jm}(\boldsymbol{r}) = \sqrt{\frac{\omega}{2\pi}}\left\{\sqrt{\frac{j}{2j+1}}g_{j+1}(\omega r)\boldsymbol{Y}_{j,j+1,m}(\boldsymbol{n}) - \sqrt{\frac{j+1}{2j+1}}g_{j-1}(\omega r)\boldsymbol{Y}_{j,j-1,m}(\boldsymbol{n})\right\} \quad (7)$$

where

$$g_l(\omega r) = (2\pi)^{3/2}i^l\frac{1}{\sqrt{\omega r}}J_{l+1/2}(\omega r). \quad (8)$$

J_l is the Bessel function, and $\boldsymbol{n} \equiv \boldsymbol{r}/r$ and $\boldsymbol{Y}_{jlm}$ are the vector spherical functions.

With the normalization adopted for the photon wave function in Eq. (7) (remembering that in r.u. the variable ωr is dimensionless) we find that the matrix elements in Eq. (4) will have the dimension of length, and the amplitude $A^{\rm E1}_{1s_{1/2}(2p_{1/2})}$ will have the dimensionality of the volume, as it is necessary for the polarizability. In the nonrelativistic limit $\omega \approx m_e(\alpha Z_{\rm eff})^2$, $r \approx \frac{1}{m_e\alpha Z_{\rm eff}}$ (α is the fine-structure constant, $Z_{\rm eff}$ is the screened charge of the nucleus, as it is seen by the valence electron), and $\omega r \approx \alpha Z_{\rm eff} \ll 1$. Then, expanding Eq. (7) in the power series in ωr and keeping only the largest terms, we obtain from Eq. (4) an expression for the resonant polarizability corresponding to the process depicted in Fig. 1:

$$\alpha^{m_i m_f}(\omega) = e^2\frac{\langle ns_{1/2}|(-1)^{m_i}r^{-m_i}|n'p_{1/2}\rangle\langle n'p_{1/2}|r^{m_f}|ns_{1/2}\rangle}{E_{n'p_{1/2}} - E_{ns_{1/2}} - \omega - \frac{i}{2}\Gamma_{n'p_{1/2}}}, \quad (9)$$

where r^m are the spherical components of the radius vector $\boldsymbol{r}$. In Eq. (9) averaging is assumed over the spin components of the initial $ns_{1/2}$ states and summation over the spin components of the final $ns_{1/2}$ states. Expression (9) can be easily generalized for an arbitrary atomic valence electron configuration. Therefore, in practical calculations we employ Eq. (9), keeping relativistic expressions for one-electron wave functions and energies. Equation (9) provides an expression for the second-rank tensor of polarizability. The standard expression for the refractive index in the case of an isotropic medium (vapor) is connected with the scalar polarizability $\alpha(\omega)$ as in Eq. (2). A scalar part of the tensor Eq. (9) is obtained with $m_i = m_f = m$:

$$\alpha(\omega) = \frac{1}{3}\alpha^{mm}(\omega) = \frac{e^2}{3}\frac{\langle ns_{1/2}|\boldsymbol{r}|n'p_{1/2}\rangle\langle n'p_{1/2}|\boldsymbol{r}|ns_{1/2}\rangle}{E_{n'p_{1/2}} - E_{ns_{1/2}} - \omega - \frac{i}{2}\Gamma_{n'p_{1/2}}}. \quad (10)$$

C. Linear Stark shift caused by the $\mathcal{P},\mathcal{T}$-odd effects in atomic systems

In this section we demonstrate how the birefringence arises in atomic systems due to the $\mathcal{P},\mathcal{T}$-odd effects. As an example, we consider again an atom in the ground $ns_{1/2}$ state excited by resonance photon scattering to the $n'p_{1/2}$ state and located in an external electric field. The electric field employed for the observation of the $\mathcal{P},\mathcal{T}$-odd Faraday effect in the case of atoms should be the maximum achievable in the laboratory, i.e., about 10^5 V/cm [12]. An electric field that begins to destroy the atomic structure is of the order 10^9 V/cm [36]. Then the influence of the electric field can be considered as a perturbation in all cases except the situation when the levels of the opposite parity are too close to each other, as in hydrogen atoms. We denote the one-electron wave functions and one-electron energies as ψ_{nl} and E_{nl}, respectively. Then the refractive index in the case of resonant photon scattering in an external electric field according to Eq. (10) will look like

$$n(\omega) = 1 + \frac{2\pi}{3}\rho e^2\sum_m\frac{\langle ns_{1/2}|r^m|n'p_{1/2}\rangle\langle n'p_{1/2}|r^m|ns_{1/2}\rangle}{E_{n'p_{1/2}} - E_{ns_{1/2}} - \omega - \frac{i}{2}\Gamma_{n'p_{1/2}}}, \quad (11)$$

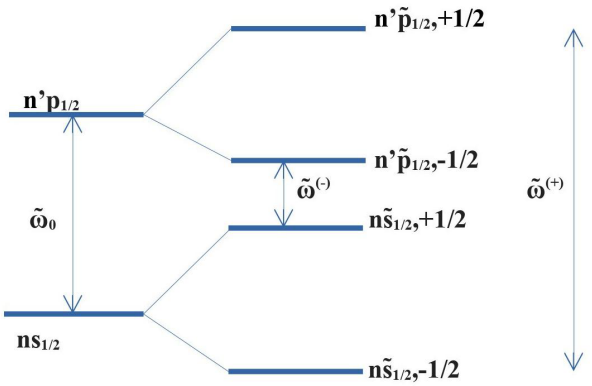

FIG. 2. Scheme of the linear Stark splitting of the levels $\widetilde{n'p}_{1/2}$ and $\widetilde{ns}_{1/2}$, where the sign $\sim$ denotes the levels corrected by electric field.

where $\Gamma_{n'p_{1/2}}$ is the level width modified by an external electric field. In an external electric field both energy levels $E_{n'p_{1/2}}$ and $E_{ns_{1/2}}$ are split into two components due to the $\mathcal{P},\mathcal{T}$-odd effects, as it is shown in Fig. 2.

In the case of absorption spectroscopy experiments (ICAS) we have to consider the absorption part of the process, Fig. 1, ignoring the behavior of the emitted photons. Then, according to Fig. 2 the absorption resonance spectral line is split in two lines with frequencies $\omega^{(+)}$ and $\omega^{(-)}$. It is assumed that the observer looks along the direction of the light propagation and opposite to this direction. Then $\omega^{(+)}$ corresponds to the absorption of the right circularly polarized photons and $\omega^{(-)}$ corresponds to the absorption of the left circularly polarized photons. The values $\omega^{(\pm)}$ are

$$\omega^{(+)} = \omega_0 + \langle n' p_{1/2,+1/2}|S|n' p_{1/2,+1/2}\rangle + \langle ns_{1/2,-1/2}|S|ns_{1/2,-1/2}\rangle, \tag{12}$$

$$\omega^{(-)} = \omega_0 + \langle n' p_{1/2,-1/2}|S|n' p_{1/2,-1/2}\rangle + \langle ns_{1/2,+1/2}|S|ns_{1/2,+1/2}\rangle, \tag{13}$$

where

$$\omega_0 = E_{n'p_{1/2}} - E_{ns_{1/2}}, \tag{14}$$

and $\langle n'l'_{1/2,m'_s}|S|nl_{1/2,m_s}\rangle$ with $m'_s, m_s = \pm 1/2$ are the linear Stark matrix elements for different linear Stark sublevels. The expressions for the Stark matrix elements are different for the different $\mathcal{P},\mathcal{T}$-odd effects. In the case of the linear Stark effect produced by the electron EDM, the Stark matrix element looks like [5]

$$\langle nl_{1/2,m_s}|S|nl_{1/2,m_s}\rangle = -d_e\langle nl_{1/2,m_s}|(\gamma_0-1)\boldsymbol{\mathcal{E}}\boldsymbol{\Sigma}|nl_{1/2,m_s}\rangle + d_e e\boldsymbol{\mathcal{E}}\sum_{n''l''_{j,m_j}}\left\{\frac{\langle nl_{1/2,m_s}|\boldsymbol{r}|n''l''_{j,m_j}\rangle\langle n''l''_{j,m_j}|(\gamma_0-1)\boldsymbol{\mathcal{E}}_c\boldsymbol{\Sigma}|nl_{1/2,m_s}\rangle}{E_{n''l''_j}-E_{nl_{1/2}}}\right.$$
$$\left.+\frac{\langle nl_{1/2,m_s}|(\gamma_0-1)\boldsymbol{\mathcal{E}}_c\boldsymbol{\Sigma}|n''l''_{j,m_j}\rangle\langle n''l''_{j,m_j}|\boldsymbol{r}|nl_{1/2,m_s}\rangle}{E_{n''l''_j}-E_{nl_{1/2}}}\right\}. \tag{15}$$

Here d_e is the absolute value of the electron EDM, $\gamma_0, \boldsymbol{\Sigma}$ are Dirac matrices, $\boldsymbol{\mathcal{E}}$ is the strength of an external electric field and $\boldsymbol{\mathcal{E}}_c$ is the strength of the Coulomb field of the nucleus and other electrons, $\boldsymbol{r}$ is the electron radius vector, and e is the electron charge. The summation in Eq. (15) runs over the entire spectrum in an atomic system. If necessary, Eq. (15) can be extended to any more advanced description of the system. The first term in the right-hand side of Eq. (15) is negligibly small [31] and can be omitted. The presence of the factor $(\gamma_0 - 1)$ in the matrix elements in Eq. (15) retains in these matrix elements only the lower components of the Dirac wave functions, i.e., the pure relativistic (magnetic) contribution. This is a consequence of the Schiff theorem which forbids the electron EDM effect for systems with only electrostatic forces acting between the particles [37]. Then the linear Stark matrix element can be expressed in the following way:

$$\langle nl_{1/2,m_s}|S|nl_{1/2,m_s}\rangle = R_d d_e \mathcal{E}. \tag{16}$$

Equations (15) and (16) define the enhancement coefficient R_d of the electron EDM in an atom. Note also that according to [38] within the Dirac-Coulomb Hamiltonian one can use an alternative expression for the $\mathcal{P},\mathcal{T}$-odd interaction:

$$V^{e\mathrm{EDM}} = d_e\frac{2i}{e\hbar}c\gamma^0\gamma^5\boldsymbol{p}^2, \tag{17}$$

where $\boldsymbol{p}$ is the momentum operator for an electron. The advantage of this form of the interaction is that it is one electron.

In a similar way the linear Stark matrix element for the case of the $\mathcal{P},\mathcal{T}$-odd electron-nucleus interaction in an external electric field can be derived [11]:

$$\langle nl_{1/2,m_s}|S|nl_{1/2,m_s}\rangle = \sum_{n''l''_{j,m_j}}\left\{\frac{\langle nl_{1/2,m_s}|\boldsymbol{r}|n''l''_{j,m_j}\rangle\langle n''l''_{j,m_j}|V_{\mathcal{P},\mathcal{T}}|nl_{1/2,m_s}\rangle}{E_{n''l''_j}-E_{nl_{1/2}}}\right.$$
$$\left.+\frac{\langle nl_{1/2,m_s}|V_{\mathcal{P},\mathcal{T}}|nl_{1/2,m_s}\rangle\langle n''l''_{j,m_j}|\boldsymbol{r}|nl_{1/2,m_s}\rangle}{E_{n''l''_j}-E_{nl_{1/2}}}\right\}. \tag{18}$$

Here $V_{\mathcal{P},\mathcal{T}}$ is the operator of the effective $\mathcal{P},\mathcal{T}$-odd electron-nucleus interaction [10,11]

$$V_{\mathcal{P},\mathcal{T}} = Q_{\mathcal{P},\mathcal{T}}C_S i\frac{G_F}{\sqrt{2}}\gamma_0\gamma_5\rho(\boldsymbol{r}), \tag{19}$$

where C_S is the electron-nucleon coupling coefficient, G_F is the Fermi-coupling constant, and $Q_{\mathcal{P},\mathcal{T}}$ is the "$\mathcal{P},\mathcal{T}$-odd charge of the nucleus." In both models of the $\mathcal{P},\mathcal{T}$-odd electron-nucleus interaction [21,22] mentioned in the Introduction, $Q_{\mathcal{P},\mathcal{T}} = A$, where A is the atomic number. $\rho(\boldsymbol{r})$ is the normalized nuclear density. Then the linear Stark matrix

element can be expressed in the following way:

$$\langle nl_{1/2,m_s}|S|nl_{1/2,m_s}\rangle = C_S R_S \mathcal{E}. \tag{20}$$

Equations (18) and (20) define the constant R_S. Comparison of Eqs. (16) and (20) interprets the EDM of an atom in terms of the C_S constant and vice versa.

III. $\mathcal{P},\mathcal{T}$-ODD FARADAY ROTATION ANGLE

A. $\mathcal{P},\mathcal{T}$-odd Faraday rotation line shape

From Eqs. (1), (2), and (11) an expression follows for the $\mathcal{P},\mathcal{T}$-odd Faraday rotation angle in the absorption experiment:

$$\psi(\omega) = \frac{2\pi^2}{3}\frac{l}{\lambda}\rho e^2 \sum_m \langle ns_{1/2}|r^m|n'p_{1/2}\rangle\langle n'p_{1/2}|r^m|ns_{1/2}\rangle \times \left\{\frac{\omega^{(+)}-\omega}{(\omega^{(+)}-\omega)^2+\frac{1}{4}\Gamma^2_{n'p_{1/2}}} - \frac{\omega^{(-)}-\omega}{(\omega^{(-)}-\omega)^2+\frac{1}{4}\Gamma^2_{n'p_{1/2}}}\right\}. \tag{21}$$

When discussing the resonant $\mathcal{P},\mathcal{T}$-odd Faraday effect an important question about the spectral line shape for this effect should be considered. The spectral line shape for the resonant $\mathcal{P}$-odd optical rotation effect (as well as for the natural optical activity effect) is antisymmetric with respect to the resonant frequency point, while the absorption line shape is symmetric with respect to this point and drops down fast towards the wings of the line. This allows one to work off resonance, where the absorption is small, and to use a large optical path length, as it was suggested in Ref. [27]. The situation with the $\mathcal{P},\mathcal{T}$-odd Faraday effect as well as with the ordinary Faraday effect is different. The spectral line shape in this case is symmetric with respect to the position of the resonance frequency exactly as the absorption line shape. This causes the problem of avoiding absorption when observing the $\mathcal{P},\mathcal{T}$-odd Faraday effect. Below we examine this problem in more detail.

For any kind of birefringence (caused by the natural optical activity, the $\mathcal{P}$-odd optical activity, the ordinary Faraday effect, or the $\mathcal{P},\mathcal{T}$-odd Faraday effect) the rotation angle ψ is proportional to $\mathrm{Re}(n^+ - n^-)$ [see Eq. (1)]. In case of the $\mathcal{P}$-odd optical rotation this difference is defined by $\mathrm{Re}[n^+(\omega) - n^-(\omega)] = 4\mathcal{P}[\mathrm{Re}n(\omega) - 1]$, where $\mathcal{P}$ is the degree of the parity nonconservation. Then the line shape is antisymmetric with respect to the resonant frequency ω_0. In the case of a Faraday effect (ordinary or $\mathcal{P},\mathcal{T}$-odd) we can expand $n^{\pm}(\omega)$ in terms of the external magnetic or electric fields,

$$\mathrm{Re}\left(n^{(+)} - n^{(-)}\right) = \frac{d}{d\omega}\mathrm{Re}(n(\omega))\langle \boldsymbol{\mu_e}\boldsymbol{\mathcal{H}}\rangle \tag{22}$$

for the ordinary Faraday effect, and

$$\mathrm{Re}(n^{(+)} - n^{(-)}) = \frac{d}{d\omega}\mathrm{Re}(n(\omega))\langle \boldsymbol{d_e}\boldsymbol{\mathcal{E}}\rangle \tag{23}$$

for the $\mathcal{P},\mathcal{T}$-odd Faraday effect. In Eqs. (22) and (23), $\boldsymbol{\mu_e}$ and $\boldsymbol{d_e}$ are the magnetic and electric dipole moments of an electron, $\boldsymbol{\mathcal{H}}$ and $\boldsymbol{\mathcal{E}}$ are the magnetic and electric field strengths, and $\langle \boldsymbol{\mu_e}\boldsymbol{\mathcal{H}}\rangle$ and $\langle \boldsymbol{d_e}\boldsymbol{\mathcal{E}}\rangle$ denote the average values for the Zeeman and linear Stark shifts, respectively. The smallness of the $\mathcal{P},\mathcal{T}$-odd Faraday effect is defined by the smallness of d_e compared to μ_e. In the Gauss system of the electromagnetic units the dipole moments μ_e and d_e are of the same dimensionality (as well as magnetic and electric fields). In units of e cm the Bohr magneton $\mu_0 = \mu_e$ equals

$$\mu_e = 1.68\times 10^{-11}\, e\,\mathrm{cm}. \tag{24}$$

The largest prediction for d_e in SM (see Introduction) is

$$d_e \approx 10^{-38}\, e\,\mathrm{cm}. \tag{25}$$

From Eqs. (22) and (23) it follows that line shapes for the Faraday effect are symmetric with respect to the value ω_0.

For further discussion we follow the derivations in [31], where a similar problem was considered for the $\mathcal{P}$-odd optical rotation. In general, $n(\omega)$ is a complex function. Its real (dispersive) part describes the dependence of the $\mathcal{P}$-odd optical rotation angle (as well as the natural optical activity) on the light frequency in the vicinity of the resonance. The imaginary (absorptive) part of $n(\omega)$ defines the absorption coefficient (absorption length). In the real situation for the light propagating through an atomic vapor with collisional broadening taken into account the function $n(\omega)$ is defined as the convolution of the Lorentz profile with Maxwell distribution of atomic velocities (Voigt profile). For simplicity we neglect the natural linewidth compared to the Doppler width. This corresponds to the standard real situation. Then with the parametrization adopted in [31] Re $n(\omega)$ and hence the behavior of the rotation angle for $\mathcal{P}$-odd optical activity is proportional to

$$\mathrm{Re}\ n(\omega) \approx \mathrm{Im}\ \mathcal{F}(u,v) \equiv g(u,v), \tag{26}$$

and the absorptive part is proportional to

$$\mathrm{Im}\ n(\omega) \approx \mathrm{Re}\ \mathcal{F}(u,v) \equiv f(u,v), \tag{27}$$

where

$$\mathcal{F}(u,v) = \sqrt{\pi}e^{-(u+iv)^2}\{1 - \mathrm{erf}[-i(u+iv)]\}. \tag{28}$$

In Eq. (28) erf(z) is the error function, and the dimensionless variable u is defined as a ratio

$$u = \frac{\Delta\omega}{\Gamma_D}, \tag{29}$$

where $\Delta\omega$ is the detuning of the frequency and Γ_D is the Doppler width. The Doppler width is defined as [27]

$$\Gamma_D = \omega_0\sqrt{\frac{2k_BT}{Mc^2}}, \tag{30}$$

where k_B is the Boltzmann constant, T is the vapor temperature in Kelvin, M is the mass of an atom, and c is the speed of the light. The dimensionless variable v is defined as a ratio

$$v = \frac{\Gamma}{2\Gamma_D}. \tag{31}$$

Here Γ is the collisional broadening width and

$$\frac{\Gamma}{2} \approx \rho\sigma_{\mathrm{col}}\sqrt{\frac{2k_BT}{M}}, \tag{32}$$

where ρ is the vapor number density and σ_{col} is the collisional cross section.

The behavior of the functions $g(u)$ and $f(u)$ with $v \ll 1$ is presented in Figs. 3(a) and 3(b), respectively.

In Fig. 3(c) the function $h(u) = \frac{dg}{du}$ with $v \ll 1$ is presented. This function represents the behavior of rotation angle caused

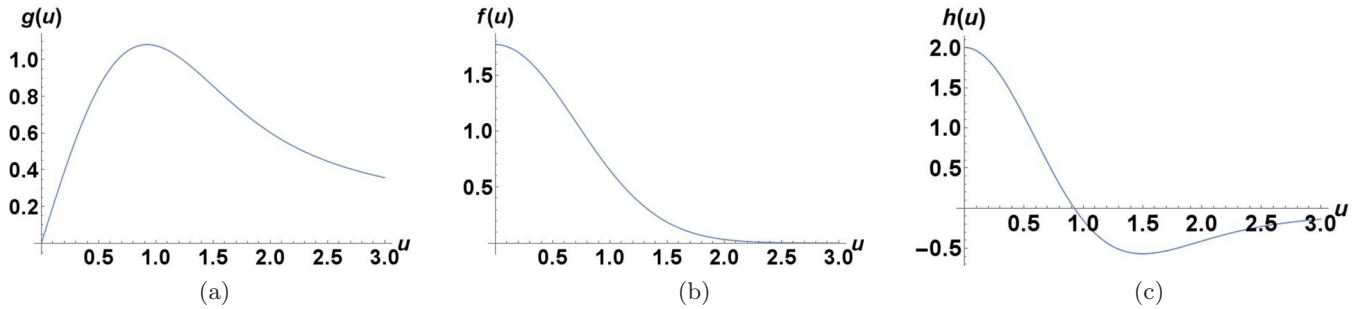

FIG. 3. Behavior of the functions $g(u)$, $f(u)$, and $h(u)$ with $v \ll 1$ close to resonance: (a) behavior of the rotation angle for optical rotation (natural or $\mathcal{P}$ odd), (b) L_0^{-1}, where L_0 is the absorption length, and (c) the rotation angle for the Faraday effect (ordinary or $\mathcal{P},\mathcal{T}$-odd).

by the Faraday (ordinary or $\mathcal{P},\mathcal{T}$-odd) effect close to the resonance frequency. As it can be seen from Fig. 3(c), this function has two maxima (by absolute value): one maximum at the point of resonance, coinciding with the maximum of absorption, and another maximum off the resonance where absorption is small. This second maximum should allow one to work off-resonance when observing the ordinary Faraday effect or searching for the $\mathcal{P},\mathcal{T}$-odd Faraday effect with large optical path length.

The result, Eq. (22) is well known (see, for example, Eq. (3) in [39]). However, when discussing the ordinary Faraday effect, the existence of the second maximum is not important. Usually the optical path length necessary to observe the ordinary Faraday rotation is smaller than the absorption length. So normally the Faraday effect drops down away from the resonance point and even turns to zero at the detuning equal to $\Delta\omega \approx 1\Gamma_D$, which coincides with the maximum of the optical activity rotation [see Fig. 3(a)]. Figure 3(c) shows that further from the resonance the Faraday rotation should grow (by modulus) again and reaches the second maximum at $\Delta\omega \approx 1.5\Gamma_D$. The existence of the second maximum is crucially important for observation of the tiny $\mathcal{P},\mathcal{T}$-odd Faraday effect, when the necessary optical path length should be many times larger than the absorption length $L(\omega_0)$.

Now we present the result Eq. (21) in the form Eq. (23), convolute it with the Maxwell distribution of atomic velocities, and take into account the Doppler broadening. Extending an approach applied in [31] for description of the $\mathcal{P}$-odd rotation to the case of $\mathcal{P},\mathcal{T}$-odd Faraday rotation we find

$$\psi(\omega) = \frac{2\pi^2}{3}\frac{l}{\lambda}\rho e^2|\langle ns_{1/2}|\boldsymbol{r}|n'p_{1/2}\rangle|^2\frac{1}{\Gamma_D} \times h(u,v) \times \frac{\omega^{(+)}-\omega^{(-)}}{\Gamma_D}. \tag{33}$$

Here we have used that $\frac{1}{\Gamma_D}\frac{d}{du} = \frac{d}{d\omega}$. Equation (33) represents the $\mathcal{P},\mathcal{T}$-odd Faraday rotation line shape.

B. $\mathcal{P},\mathcal{T}$-odd Faraday rotation signal

Not only the magnitude of rotation angle, but also an amount of the light transmitted to the point of detection is important for performing the Faraday experiment. Following [27] we call the product of the angle $\psi(\omega)$ and transmitted function $T(\omega)$ the signal $R(\omega)$:

$$R(\omega) = \psi(\omega)T(\omega). \tag{34}$$

The transmission function is defined by the Beer-Lambert law:

$$T(\omega) = e^{-D(\omega)}, \tag{35}$$

where $D(\omega)$ is the optical depth. This depth is defined as

$$D(\omega) = \frac{l}{L(\omega)}. \tag{36}$$

Here l is the optical path length and $L(\omega)$ is the absorption length:

$$L^{-1}(\omega) = \rho\sigma(\omega), \tag{37}$$

and $\sigma(\omega)$ is the absorption cross section for the light propagating through a medium. The cross section $\sigma(\omega)$ for transitions of E1 type can be presented like [31]

$$\sigma(\omega) = 4\pi\frac{\omega_0}{\Gamma_D}f(u,v)\frac{e^2|\langle ns_{1/2}|\boldsymbol{r}|n'p_{1/2}\rangle|^2}{3\hbar c}. \tag{38}$$

This formula follows from the optical theorem [40]

$$\mathrm{Im}A(0) = \frac{\omega}{4\pi}\sigma, \tag{39}$$

where $A(0)$ is the light elastic scattering amplitude for zero angle and σ is the total cross section. For the resonance case σ can be understood as an absorption cross section. Then we have to take into account the relation between the scattering amplitude and polarizability $\alpha(\omega)$ as described in Sec. II B also for the case of resonance.

The next step is to find the optimal value $u = u_{\mathrm{opt}}$ and $\rho = \rho_{\mathrm{opt}}$ at which the signal R has its maximum with the fixed parameter l. Then by inserting this value in Eqs. (33), (34), and (35) an expression for the maximum rotation signal as a function of l can be obtained,

$$R_{\max}(l) = \frac{2\pi^2}{3}\frac{l}{\lambda}\rho_{\mathrm{opt}}e^2|\langle ns_{1/2}|\boldsymbol{r}|n'p_{1/2}\rangle|^2\frac{1}{\hbar\Gamma_D} \times h(u_{\mathrm{opt}})\frac{\omega^{(+)}-\omega^{(-)}}{\Gamma_D}e^{-\rho_{\mathrm{opt}}\sigma(\omega_{\mathrm{opt}})l}, \tag{40}$$

where

$$\omega_{\mathrm{opt}} = \omega_0 + \Delta\omega_{\mathrm{opt}} = \omega_0 + \Gamma_D u_{\mathrm{opt}}(l). \tag{41}$$

Equation (40) is a final expression for calculating the $\mathcal{P},\mathcal{T}$-odd Faraday rotation signal. For this calculation we have to fix a particular transition in an atom, and then the value of λ will be also fixed. A natural choice of the transition is an E1 transition $ns_{1/2} \to n'p_{1/2}$, as it was supposed above. In this

case the value of the rotation angle is the largest. However, M1 transitions $ns_{1/2} \to n's_{1/2}, np_{1/2} \to n'p_{1/2}, n'p_{3/2}$ also can be used. For these transitions the transmission of the light is larger than for E1 transitions. In the case of $np_{1/2} \to n'p_{3/2}$ transitions the satellite E2 transitions should be taken into account. These transitions do not influence the value of the rotation angle but diminish the light transmission due to the additional absorption. In the case of M1 transitions between p states the factor $e^2|\langle ns_{1/2}|\boldsymbol{r}|n'p_{1/2}\rangle|^2$ should be replaced by

$$e^2|\langle ns_{1/2}|\boldsymbol{r}|n'p_{1/2}\rangle|^2 \to \mu_0^2|\langle np_{1/2(3/2)}|\boldsymbol{l} - g_S\boldsymbol{s}|n'p_{1/2(3/2)}\rangle|^2, \tag{42}$$

where $\boldsymbol{s}, \boldsymbol{l}$ are the spin and orbital angular momenta operators for an electron, respectively, $g_S = 2.0023$ is a free-electron g factor, and μ_0 is the Bohr magneton. Also, the expression Eq. (38) for $\sigma(\omega)$ should be replaced by

$$\sigma(\omega) = 4\pi\frac{\omega_0}{\Gamma_D}f(u,v)\frac{\mu_0^2|\langle np_{1/2(3/2)}|\boldsymbol{l} - g_S\boldsymbol{s}|n'p_{1/2(3/2)}\rangle|^2}{3\hbar c}. \tag{43}$$

Finally, the choice of the parameters ρ, Γ_D depends on the conditions of the particular experiments.

In the next sections we present the accurate calculations of the dependence of $R_{\max}(l)$ on l for several atoms, demonstrating the possibility to use the $\mathcal{P},\mathcal{T}$-odd Faraday experiment for the observation of the electron EDM.

In all the derivations above we neglected the hyperfine splitting of the levels $ns_{1/2}$ and $n'p_{1/2}$. With the hyperfine interaction taken into account, both these levels are split in two hyperfine levels with the total atomic angular momenta $F = I + 1/2$ and $F = I - 1/2$, where I is the nuclear spin. In an external magnetic field or in an external electric field when $\mathcal{P},\mathcal{T}$-odd effects are included, both these hyperfine levels are split in $2(I + 1/2) + 1$ or $2(I - 1/2) + 1$ components, respectively. Among the transitions between two sets of sublevels for $ns_{1/2}$ and $np_{1/2}$ levels there are transitions with the right and left circularly polarized photons. However, the total intensities of the right and left circularly polarized transitions are equal to the intensity of the right and left transitions between the levels $ns_{1/2}$ and $n'p_{1/2}$ in external fields without the hyperfine splitting. Therefore if in the experiment the hyperfine structure of atomic levels is not resolved one can use all the preceding formulas for the evaluation of $\mathcal{P},\mathcal{T}$-odd effects. In particular, Eqs. (12) and (13) remain valid, and the expressions for the polarizability Eq. (10) and absorption cross section Eq. (38) also remain valid. When the hyperfine structure is resolved and the transitions between the hyperfine sublevels of different electronic levels are considered, all formulas above can be easily generalized using the standard techniques for the hyperfine interaction. For example, the hyperfine splitting of arbitrary atomic levels and expressions for arbitrary electron operators with account for hyperfine interactions can be found in [41].

IV. ELECTRONIC STRUCTURE CALCULATION DETAILS

Direct use of Eqs. (15) and (18) corresponds to the so-called sum over states method. Formally, the summation in the equations should include all the excited states. In practice, only several contributions to this sum are taken into account. However, it is possible to reformulate the problem: instead of explicit summation of the second-order perturbation theory expression one can calculate expression (15) as the mixed derivative of the energy with respect to the external electric field and d_e [42,43]. Note that in Ref. [43] the approach ("strategy I") where one adds the interaction with the external electric field already at the self-consistent field stage of calculation was formulated.

To calculate Stark shifts in the ground and excited electronic states of Cs, Tl, Pb, and Ra we used the Fock-space coupled cluster with single- and double-cluster amplitudes method [44] to treat electron correlation effects. $1s..3d$ electrons were excluded from the treatment. Dyall's all-electron triple-zeta (AETZ) [45,46] basis sets were used in the calculations augmented by diffuse functions from the augmented core valence triple-zeta (ACVTZ) basis sets [45,46].

E1 and M1 transition matrix elements were calculated using the multireference linear-response coupled cluster with single- and double-amplitudes method [47–49]. For these calculations

TABLE I. Enhancement coefficients R_d for the electron EDM effect for different atoms and the states under consideration and the linear Stark shifts for the states in an external electric field $\mathcal{E} = 100$ kV/cm [12] corresponding to the present electron EDM bound established in experiments with ThO molecules [14].

Atom	State	R_d	Linear Stark shift, 10^{-20} eV
Cs	$6s_{1/2,+1/2}$	107	0.096
	$6p_{1/2,+1/2}$	−194	−0.17
Tl	$6p_{1/2,+1/2}$	−526	−0.47
	$6p_{3/2,+1/2}$	7	0.006
Pb	$6p^2(1/2,1/2)_0$	0	0
	$6p7s(1/2,1/2)_{+1}$	844	0.76
	$6p^2(3/2,1/2)_{+1}$	234	0.21
Ra	$6p^27s^2, {}^1S_0$	0	0
	$6p^27s7p, {}^3P_{1,+1}$	−1595	−1.4

TABLE II. The enhancement factors R_S for the $\mathcal{P},\mathcal{T}$-odd electron-nucleus interaction effect for different atoms and the states under consideration and the linear Stark shifts of the states in an external electric field $\mathcal{E} = 100$ kV/cm [12] corresponding to the present C_S bound established in experiments with ThO molecules [14] ($C_S = 5.9\times10^{-9}$).

Atom	State	R_S, $10^{-17}e$ cm	Linear Stark shift, 10^{-20} eV
Cs	$6s_{1/2,+1/2}$	0.0662	0.039
	$6p_{1/2,+1/2}$	−0.12	−0.071
Tl	$6p_{1/2,+1/2}$	−0.64	−0.38
	$6p_{3/2,+1/2}$	0.0071	0.006
Pb	$6p^2(1/2,1/2)_0$	0	0
	$6p7s(1/2,1/2)_{+1}$	1.04	0.61
	$6p^2(3/2,1/2)_{+1}$	0.285	0.17
Ra	$6p^27s^2, {}^1S_0$	0	0
	$6p^27s7p, {}^3P_{1,+1}$	−2.17	−1.3

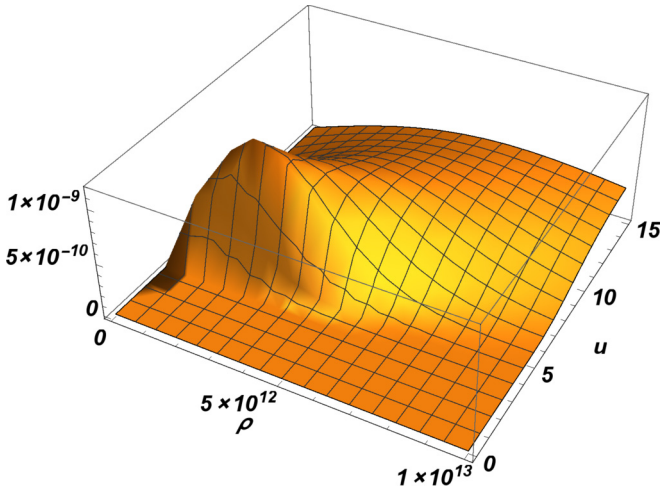

FIG. 4. The dependence of the $\mathcal{P},\mathcal{T}$-odd Faraday signal R (in rad) on the dimensionless detuning u and on the vapor density ρ (in cm^{-3}) for the E1 transition $6s_{1/2} \to 6p_{1/2}$ in a Cs atom. The optical path length l is assumed to be equal to 100 km.

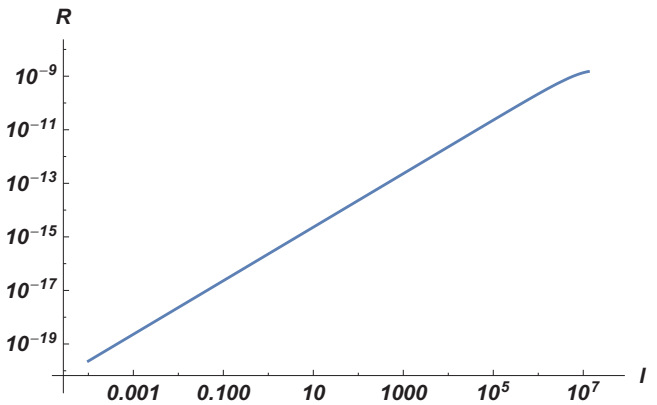

FIG. 6. Dependence of $R_{\max}(l)$ on the transition $6s_{1/2} \to 6p_{1/2}$ in a Cs atom. On the horizontal axis the optical path length is plotted in centimeters. On the vertical axis the $\mathcal{P},\mathcal{T}$-odd Faraday rotation signal is plotted in rad assuming a fixed number density $\rho_{\mathrm{opt}} = 2\times10^{12}\ \mathrm{cm}^{-3}$.

Dyall's augmented valence double-zeta (AVDZ) basis set [45,46] with additional diffuse functions was used in the case of Pb and Tl. For Cs and Ra we used the Dyall's all-electron double-zeta (AEDZ) basis set [45,46]. $1s..3d$ electrons were excluded from the correlation treatment of Cs, while $1s..4f$ were excluded from the correlation treatment of Tl, Pb, and Ra.

Electronic calculations were performed within the DIRAC12 [50] and MRCC [51] codes. Matrix elements of operators of E1,M1 transitions and $\mathcal{P},\mathcal{T}$-odd interactions were calculated using code developed in Refs. [43,52,53].

The uncertainty of the calculations can be estimated as 15%, which is sufficient for the present purpose. For example, the electron EDM enhancement coefficient for the ground state of Tl (see below) agrees within 8% with previous studies [54–56] where benchmark calculations of the coefficient have been performed.

V. NUMERICAL RESULTS AND DISCUSSION

A. Cs atom $Z = 55$

In the case of Cs the transition $6s_{1/2} \to 6p_{1/2}$ (see Fig. 2 with $n = n' = 6$) and $\lambda = 895$ nm seems to be most favorable for the observation of the $\mathcal{P},\mathcal{T}$-odd effects. The evaluation of $(\omega^{(+)} - \omega^{(-)})$ according to the formulas Eqs. (12) and (13) results in

$$(\omega^{(+)} - \omega^{(-)}) = 174\times d_e\mathcal{E} \approx 1.5\times10^{-21}\ e\mathrm{V}, \qquad (44)$$

where for an electron EDM d_e we put the value established in experiment with a ThO molecule [14] ($d_e = 0.9\times10^{-28}\ e\,\mathrm{cm}$) and for an external electric field we set $\mathcal{E} = 10^5$ V/cm. See Table I for the enhancement coefficients R_d for the electron EDM effect and the corresponding linear Stark shifts. Also see the Table II for the enhancement factors R_S for the $\mathcal{P},\mathcal{T}$-odd electron-nucleus interaction effect and the corresponding linear Stark shifts. In what follows for estimates of the $\mathcal{P},\mathcal{T}$-odd signal R we use the values from the Table I. Analogously, this can be done also for the $\mathcal{P},\mathcal{T}$-odd electron-nucleus interaction effect.

For the Γ_D we employ the characteristic value $\Gamma_D \approx 10^{-6}\omega_0$ [31]. Let us estimate the value of the collisional broadening Γ according to Eq. (32). The characteristic value for the collisional cross section is $\sigma_{\mathrm{col}} \approx 0.5\times10^{-14}\ \mathrm{cm}^2$, and the standard temperature for the experiments with the vapors of heavy atoms is about $\sim10^3$ K. Then for the value of the atom vapor density ρ we obtain $\Gamma/2 = 2\times10^{-10}\rho[\mathrm{cm}^{-3}]\ \mathrm{s}^{-1}$. So in this case dimensionless $v = \frac{\Gamma}{2\Gamma_D} \approx 10^{-19}\rho[\mathrm{cm}^{-3}]$. Using

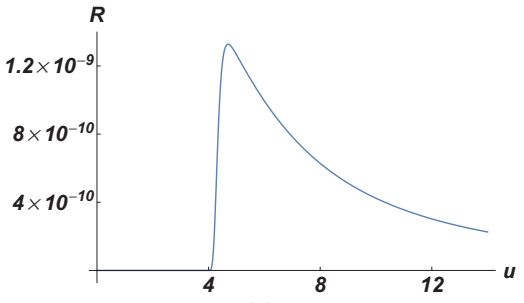

(a)

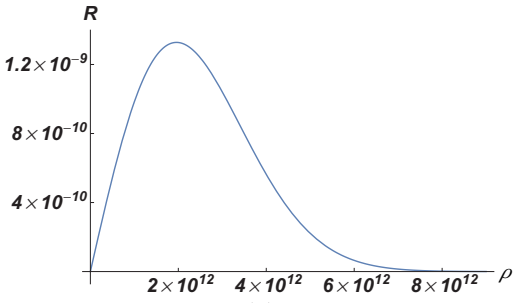

(b)

FIG. 5. (a) Behavior of the $R(u,\rho_{\mathrm{opt}})$ projection of Fig. 4 (in rad) assuming fixed number density $\rho_{\mathrm{opt}} = 2\times10^{12}\ \mathrm{cm}^{-3}$, and (b) the behavior of the $R(u_{\mathrm{opt}},\rho)$ projection of Fig. 4 (in rad) assuming fixed dimensionless detuning $u_{\mathrm{opt}} = 4.7$ (ρ in cm^{-3}).

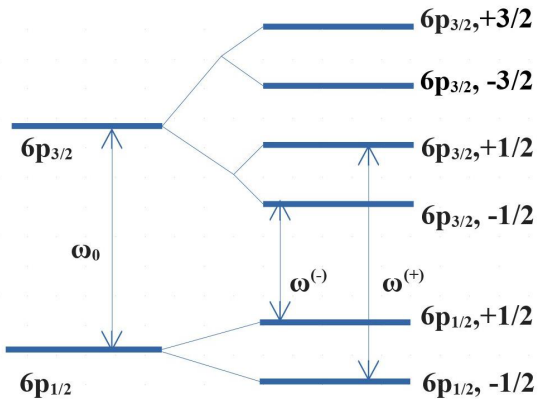

FIG. 7. Scheme of the linear Stark splitting for the transition $6p_{1/2} \to 6p_{3/2}$.

the optical path $l = 100$ km [27], our calculation, according to Eq. (40), gives the dependence $R(u,\rho)$ depicted in Fig. 4. Then it follows from Fig. 4 that the optimal number density of Cs atom vapors for the above conditions is $\rho_{\rm opt} = 2\times10^{12}$ cm^{-3} and $u_{\rm opt} = 4.7$, which gives the maximum value of the effect. $R(u,\rho_{\rm opt})$ and $R(u_{\rm opt},\rho)$ projections of Fig. 4 are presented in Figs. 5(a) and 5(b), respectively.

Then

$$R_{\rm max}(l = 100\,{\rm km}) \approx 1.4\times10^{-9}\,{\rm rad} \tag{45}$$

for the observation of the electron EDM of the order $d_e = 10^{-28}\,e$ cm.

The calculation also gives the dependence $R(l)$ with fixed number density $\rho_{\rm opt} = 2\times10^{12}$ cm^{-3} depicted in Fig. 6. For small l values the dependence $R(l)$ is linear, as it can be seen immediately from Eq. (40). For large l values this dependence becomes close to the square root $R \approx \sqrt{l}$ as it was obtained for the optical $\mathcal{P}$-odd activity with theoretical simulations in [27]. This result shows that the $\mathcal{P},\mathcal{T}$-odd rotation angle $\psi \approx 10^{-9}$ rad can be obtained with the ICAS experiment by the optical path length $l \approx 100$ km. The detection of such an angle

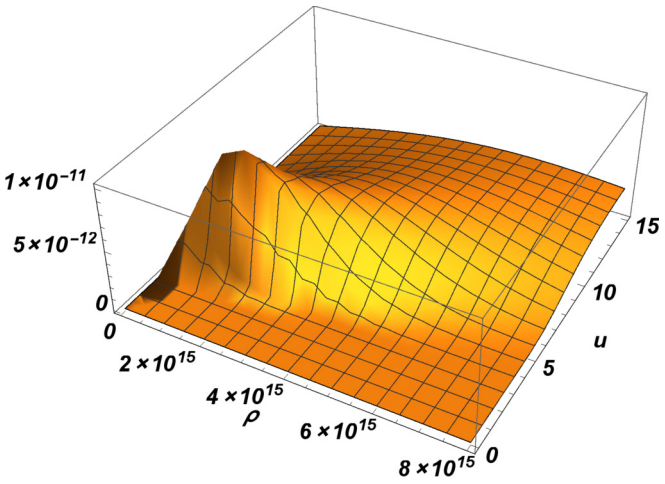

FIG. 8. Dependence of the $\mathcal{P},\mathcal{T}$-odd Faraday signal R (in rad) on dimensionless detuning u and on vapor density ρ (in cm^{-3}) for the M1 transition $6p_{1/2} \to 6p_{3/2}$ in Tl atoms. The optical path length l is assumed to be equal to 100 km.

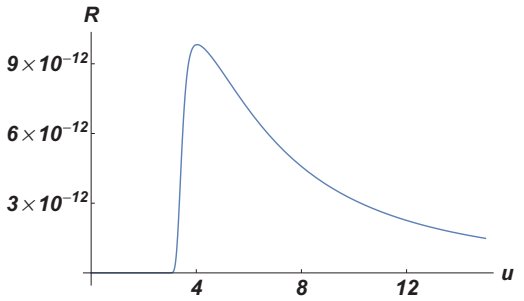

FIG. 9. Behavior of the $R(u,\rho_{\rm opt})$ projection of Fig. 8 (in rad) assuming a fixed number density $\rho_{\rm opt} = 2\times10^{15}$ cm^{-3}.

would confirm the bound for the electron EDM of the order $10^{-28}\,e$ cm. Up to date using a cavity-enhanced technique [27], the signals of about 10^{-7} rad are available. One should mention also that the record birefringence phase-shift value measured in another ICAS experiment [28] is 3×10^{-13} rad.

B. Tl atom $Z = 81$

The ground electronic configuration of Tl atoms is $6s^2 6p$. To demonstrate another possible choice of atomic transition we choose the M1 transition $6p_{1/2} \to 6p_{3/2}$. The level splitting scheme for transition $6p_{1/2} \to 6p_{3/2}$ is more complicated and is depicted in Fig. 7. An external electric field, unlike the magnetic field, produces the splitting of the atomic level momenta projections only by modulus, not by sign. The sign splitting in an external electric field occurs only due to the $\mathcal{P},\mathcal{T}$-odd linear Stark effect (see Fig. 7). In the strong electric field of the order 10^5 V/cm the splitting between $6p_{3/2}\ \pm 3/2$ projections and $6p_{3/2}\ \pm 1/2$ projections should be larger than the hyperfine structure and well distinguishable in the experiment. Then the $\mathcal{P},\mathcal{T}$-odd Faraday experiment can be performed on the transition $6p_{1/2,\pm1/2} \to 6p_{3/2,\pm1/2}$, as it is shown in Fig. 7. This transition is of M1 type. (See discussion in Sec. III about the advantages and disadvantages of using E1 and M1 transitions in $\mathcal{P},\mathcal{T}$-odd Faraday experiments.) The wavelength for this transition is $\lambda = 1283$ nm. In case of transition $6p_{1/2} \to 6p_{3/2}$, apart from M1 the E2 transition also takes place. This E2 transition does not contribute to the $\mathcal{P},\mathcal{T}$-odd Faraday rotation angle but contributes in principle to the

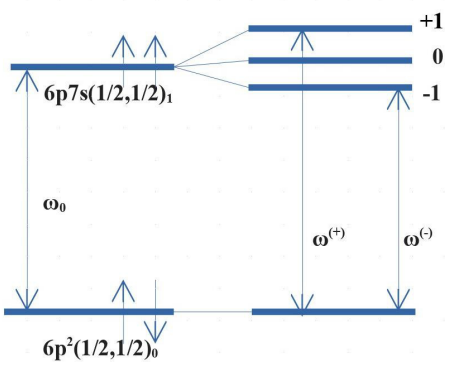

FIG. 10. Scheme of the linear Stark splitting for the transition $6p^2(1/2,1/2)_0 \to 6p7s(1/2,1/2)_1$. Short up and down arrows denote the mutual directions of the electron spins.

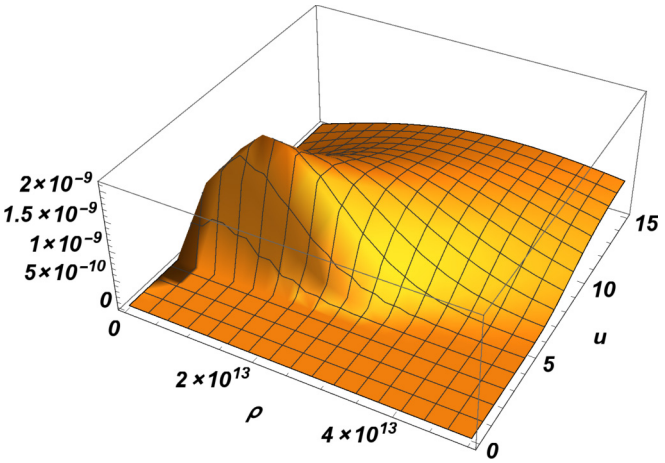

FIG. 11. Dependence of the $\mathcal{P},\mathcal{T}$-odd Faraday signal R (in rad) on the dimensionless detuning u and on the vapor density ρ (in cm^{-3}) for the E1 transition $6p^2(1/2,1/2)_0 \to 6p7s(1/2,1/2)_1$ in a Pb atom. The optical path length l is assumed to be equal to 100 km.

absorption. In this paper we neglect the E2 contribution to the absorption in the proposed $\mathcal{P},\mathcal{T}$-odd Faraday experiment. This contribution should be of the same order as the M1 contribution for the transitions $6p_{1/2} \to 6p_{3/2}$. Then, according to Eq. (40) the total $\mathcal{P},\mathcal{T}$-odd Faraday signal can be diminished. However, the M1 and E2 contributions should be additive and of the same sign, so that the change of the total $\mathcal{P},\mathcal{T}$-odd signal with inclusion of E2 absorption should not be drastic.

Necessary values for the estimate of the $\mathcal{P},\mathcal{T}$-odd Faraday signal were calculated and also quoted in Tables I and II. Similar to the Cs atom case, we perform an estimate of the $\mathcal{P},\mathcal{T}$-odd Faraday signal. Using the optical path $l = 100$ km [27], our calculation according to Eq. (40) gives the dependence $R(u,\rho)$ depicted in Fig. 8. Then it follows from Fig. 8 that the optimal number density of Tl atom vapors for the above conditions is $\rho_{\mathrm{opt}} = 2\times10^{15}$ cm^{-3} and $u_{\mathrm{opt}} = 4.0$, which gives the maximum value of the effect. The $R(u,\rho_{\mathrm{opt}})$ projection of Fig. 8 is presented in Fig. 9.

Then

$$R_{\max}(l = 100\,\mathrm{km}) \approx 1.0\times10^{-11}\,\mathrm{rad} \tag{46}$$

for the observation of the electron EDM of the order $d_e = 10^{-28}\,e\,\mathrm{cm}$.

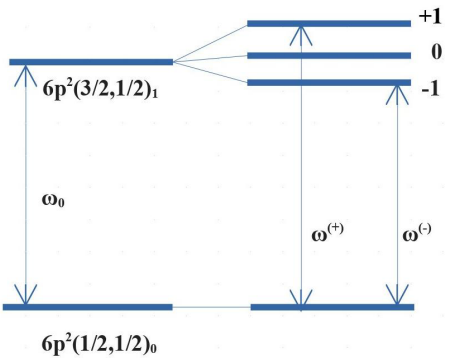

FIG. 13. Linear Stark level splitting for $6p^2(1/2,1/2)_0 \to 6p^2(3/2,1/2)_1$ transition.

C. Pb atom $Z = 82$

Here we have two possible transitions:

(1) $6p^2(1/2,1/2)_0 \to 6p7s(1/2,1/2)_1$ is of E1 type with $\lambda = 286$ nm (see Fig. 10).

Necessary values for the estimate of the $\mathcal{P},\mathcal{T}$-odd Faraday signal were calculated and also quoted in Tables I and II. Using the optical path $l = 100$ km [27], our calculation according to Eq. (40) gives the dependence $R(u,\rho)$ depicted in Fig. 11. Then it follows from Fig. 11 that the optimal number density of Pb atom vapors for the above conditions is $\rho_{\mathrm{opt}} = 1\times10^{13}$ cm^{-3} and $u_{\mathrm{opt}} = 4.6$, which gives the maximum value of the effect. $R(u,\rho_{\mathrm{opt}})$ and $R(u_{\mathrm{opt}},\rho)$ projections of Fig. 11 are presented in Figs. 12(a) and 12(b), respectively.

Then

$$R_{\max}(l = 100\,\mathrm{km}) \approx 2.5\times10^{-9}\,\mathrm{rad} \tag{47}$$

for the observation of the electron EDM of the order $d_e = 10^{-28}\,e\,\mathrm{cm}$.

(2) The $6p^2(1/2,1/2)_0 \to 6p^2(3/2,1/2)_1$ transition is of M1 type with $\lambda = 1360$ nm (see Fig. 13).

Necessary values for the estimate of the $\mathcal{P},\mathcal{T}$-odd Faraday signal were calculated and also quoted in the Tables I and II. Similar to the M1 case with a Tl atom we perform an estimate of the $\mathcal{P},\mathcal{T}$-odd Faraday signal. Using the optical path $l = 100$ km [27], our calculation according to Eq. (40) gives the dependence $R(u,\rho)$ depicted in Fig. 14. Then it follows from Fig. 14 that the optimal number density of Pb atom vapors for the above conditions is $\rho_{\mathrm{opt}} = 10^{15}$ cm^{-3} and $u_{\mathrm{opt}} = 3.7$,

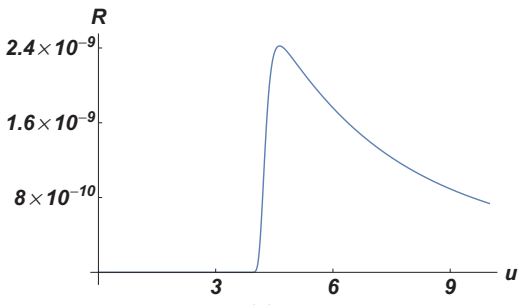

(a)

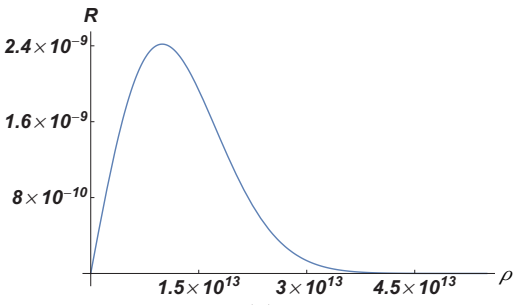

(b)

FIG. 12. (a) Behavior of the $R(u,\rho_{\mathrm{opt}})$ projection of Fig. 11 (in rad) assuming a fixed number density $\rho_{\mathrm{opt}} = 1\times10^{13}$ cm^{-3} and (b) behavior of the $R(u_{\mathrm{opt}},\rho)$ projection of Fig. 11 (in rad) assuming fixed dimensionless detuning $u_{\mathrm{opt}} = 4.6$ (ρ in cm^{-3}).

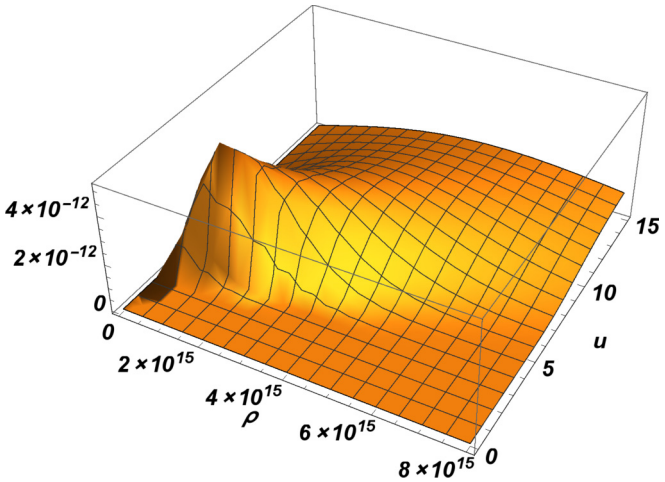

FIG. 14. Dependence of the $\mathcal{P},\mathcal{T}$-odd Faraday signal R (in rad) on the dimensionless detuning u and vapor density ρ (in cm^{-3}) for the M1 transition $6p^2(1/2,1/2)_0 \to 6p^2(3/2,1/2)_1$ in Pb atoms. The optical path length l is assumed to be equal to 100 km.

which gives the maximum value of the effect. The $R(u,\rho_{\mathrm{opt}})$ projection of Fig. 14 is presented in Fig. 15.

Then

$$R_{\max}(l = 100\,\mathrm{km}) \approx 5.8\times10^{-12}\,\mathrm{rad} \tag{48}$$

for the observation of the electron EDM of the order $d_e = 10^{-28}\,e\,\mathrm{cm}$.

D. Ra atom $Z = 88$

In this case we choose the transition $6p^27s^2,{}^1S_0 \to 6p^27s7p,{}^3P_1$ of E1 type with $\lambda = 714$ nm (see Fig. 16). Necessary values for the estimate of the $\mathcal{P},\mathcal{T}$-odd Faraday signal were calculated and also quoted in Tables I and II. Using the optical path $l = 100$ km [27], our calculation according to Eq. (40) gives the dependence $R(u,\rho)$ depicted in Fig. 17. Then it follows from Fig. 17 that the optimal number density of Ra atom vapors for the above conditions is $\rho_{\mathrm{opt}} = 1.4\times10^{13}\ \mathrm{cm}^{-3}$ and $u_{\mathrm{opt}} = 4.6$, which gives the maximum value of the effect. $R(u,\rho_{\mathrm{opt}})$ and $R(u_{\mathrm{opt}},\rho)$ projections of Fig. 17 are presented in Figs. 18(a) and 18(b), respectively.

Then

$$R_{\max}(l = 100\,\mathrm{km}) \approx 4.0\times10^{-9}\,\mathrm{rad} \tag{49}$$

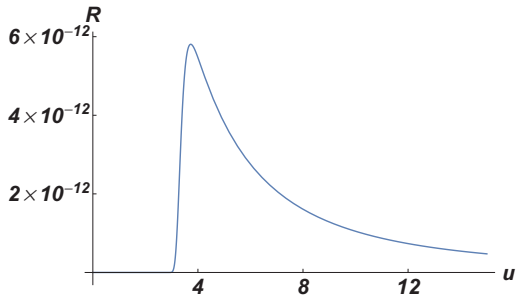

FIG. 15. Behavior of the $R(u,\rho_{\mathrm{opt}})$ projection of Fig. 14 (in rad) assuming a fixed number density $\rho_{\mathrm{opt}} = 1\times10^{15}\ \mathrm{cm}^{-3}$.

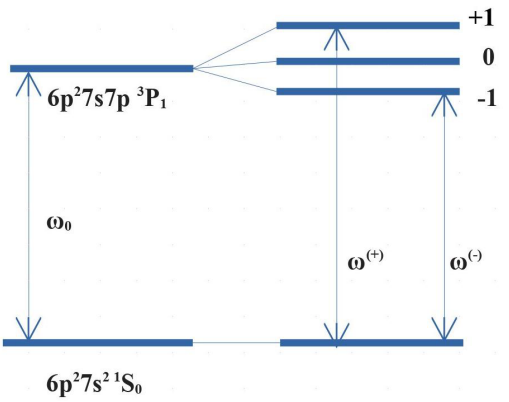

FIG. 16. $6p^27s^2,{}^1S_0 \to 6p^27s7p,{}^3P_1$.

for the observation of the electron EDM of the order $d_e = 10^{-28}\,e\,\mathrm{cm}$.

VI. CONCLUSIONS

Analyzing the data obtained in Sec. V, we conclude that it is the E1-type transitions (but not M1-type transitions) that in principle can be favorable for observation of the $\mathcal{P},\mathcal{T}$-odd Faraday effect. For path lengths of about 100 km claimed in [27] we obtained the characteristic value of the $\mathcal{P},\mathcal{T}$-odd signal $R_{\max}(l = 100\,\mathrm{km}) \approx (1-4)\times10^{-9}$ rad for the observation of the electron EDM at the level of present experiments with molecules. Concluding, we can state that none of the recent ICAS experiments can immediately provide the $\mathcal{P},\mathcal{T}$-odd Faraday study with better results than the ones already achieved in modern experiments [12–14,14]. However, there are several ways to enhance this effect within the framework of ICAS experiments. The combined power of ICAS abilities looks impressive. In [28] the optical path length of about 70 000 km in an ICAS experiment was reported. Compared to the optical path length of 100 km already claimed in [27] and used

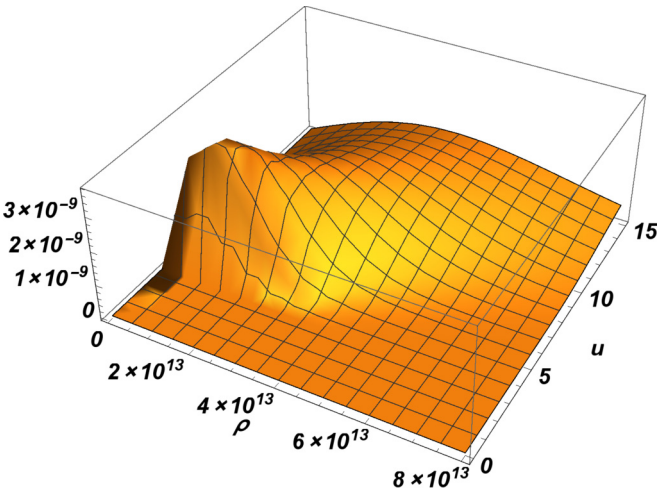

FIG. 17. Dependence of the $\mathcal{P},\mathcal{T}$-odd Faraday signal R (in rad) on dimensionless detuning u and on vapor density ρ (in cm^{-3}) for the E1 transition $6p^27s^2,{}^1S_0 \to 6p^27s7p,{}^3P_1$ in Ra atoms. The optical path length l is assumed to be equal to 100 km.

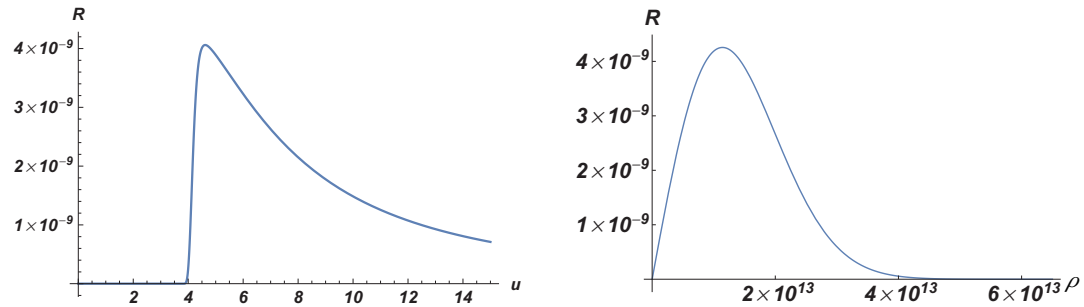

FIG. 18. (a) Behavior of the $R(u,\rho_{\rm opt})$ projection of Fig. 17 (in rad) assuming a fixed number density $\rho_{\rm opt} = 1.4\times10^{13}$ cm^{-3}, and (b) the behavior of the $R(u_{\rm opt},\rho)$ projection of Fig. 17 (in rad) assuming fixed dimensionless detuning $u_{\rm opt} = 4.6$ (ρ in cm^{-3}).

for the estimates throughout our paper, this would give a 30-times improvement of the accuracy of the electron EDM prediction in the $\mathcal{P},\mathcal{T}$-odd Faraday experiment. This follows from the established growth of the $\mathcal{P},\mathcal{T}$-odd Faraday rotation signal as $\sqrt{l}$ with the growth of the optical path length l. On the other hand, the record sensitivity 3×10^{-13} rad achieved in another ICAS experiment [29] would give another 10^4 times improvement of the EDM prediction compared to the value 4×10^{-9} rad required for fixation of EDM at the level 10^{-28} e cm according to our estimates. In total, the electron EDM of the order 0.3×10^{-33} e cm could be observed in such a combined experiment.

Another improvement of the results of the $\mathcal{P},\mathcal{T}$-odd Faraday effect measurements within the ICAS techniques may be connected with the laser cooling of the medium atoms. The Faraday rotation signal enhances with lowering of the vapor temperature T approximately as $T^{-1/2}$. Thus the cooling of the atomic vapors from the 10^3 K adopted in our estimates to 1 K (if possible) would shift the d_e bound to 10^{-35} e cm, which is not too far from the SM prediction 10^{-38} e cm.

Probably more advantageous could be the employment of molecular vapors for the search of the electron EDM with the $\mathcal{P},\mathcal{T}$-odd Faraday effect. The molecules used for this purpose in modern experiments [13,14] are necessarily free radicals. The lifetimes of diatomic free radicals in a cavity were reported to be about 5×10^{-5} s [57]. This means that the optical path length cannot exceed 15 km. Still, the diatomic molecules require a much smaller external electric field (about 1 V/cm) for obtaining the same $\mathcal{P},\mathcal{T}$-odd rotation. The enhancement coefficients are very large for these molecules (up to 10^9), which may significantly improve the present bound for the electron EDM. Another advantage of the experiments with molecules is the relative simplicity of the laser cooling.

The systematic errors in the $\mathcal{P},\mathcal{T}$-odd Faraday experiment are similar to those in the other types of the $\mathcal{P},\mathcal{T}$-odd experiments (magnetic resonance, electron spin precession in external electric field). The motional magnetic field for the chaotic motion of atoms in the cavity cannot mimic the EDM effect since it is always orthogonal to the applied electric field. The influence of the uncontrolled external static magnetic fields can be avoided if simultaneously with the measurement of the $\mathcal{P},\mathcal{T}$-odd Faraday effect the ordinary Faraday effect in the applied magnetic field parallel to the applied electric field will be measured. Then after switching the direction of the electric field the influence of the uncontrolled magnetic fields will be canceled. The danger comes only from the uncontrolled alternating magnetic fields with a frequency close to the inverse time of the electric field switching. A general problem of excluding the electromagnetic field fluctuations is considered in Appendix to this paper.

ACKNOWLEDGMENTS

In preparing the paper and the calculations of the $\mathcal{P},\mathcal{T}$-odd Faraday signals, optimal parameters for the experiments as well as E1 and M1 amplitudes were supported by the Russian Science Foundation through Grant No. 17-12-01035. The work of D.V.C. connected with the calculation of the $\mathcal{P},\mathcal{T}$-odd electron-nucleus interaction effect listed in the Table II was supported by a Foundation for the Advancement of Theoretical Physics and Mathematics "BASIS" grant according to Research Project No. 17-15-577-1. The work of L.V.S. connected with the calculation of electron EDM enhancement factors listed in Table I was supported by the RFBR through Research Project No. 16-32-60013 mol_a_dk.

APPENDIX: ESTIMATES OF THE FIELD FLUCTUATIONS IN THE $\mathcal{P},\mathcal{T}$-ODD FARADAY EXPERIMENT

Electromagnetic field fluctuations can mimic any small effect connected with the field interaction with the matter. The magnitude of any effect of this kind is proportional to the number N_e of interactions (events). However, the magnitude of the field fluctuations also grows up with N_e as $(N_e)^{1/2}$. Then, to observe a small effect of the order $\xi \ll 1$ and to distinguish the signal from the field fluctuation, it is necessary to fulfill the condition

$$N_e > \xi^{-2}. \tag{A1}$$

In case of the $\mathcal{P},\mathcal{T}$-odd Faraday effect a small measurable parameter is the rotation angle $\varphi \ll 2\pi$ of the light polarization plane. We assume that, for example, $\varphi \approx 10^{-9}$ rad, and discuss the conditions necessary to satisfy inequality (A1). The number of events N_e is the number of laser photons scattering on the atoms enclosed in the cavity during the time which is necessary for the light propagating within the cavity to cover a distance of about 100 km, i.e., 0.3×10^{-3} s. After this time the experiment has to be finished, since the light intensity will be exhausted. Let the laser beam cross section be $\sigma_b = 1$ mm^2 $= 10^{-2}$ cm^2. This beam is periodically reflected by the mirrors, and the

distance between these mirrors (the size of the cavity) we assume to be 1 m = 100 cm. The light travels from one mirror to another during the time 0.3×10^{-8} s. If we consider an excitation process of the type $ns \to n'p$, the relaxation time (the decay time) will be of the order 10^{-9} s. This means that after reflection from a mirror, the light will find all the atoms again in their ground state. Then we can estimate the full number of events during the experiment, for example,

$$N_e = N_\gamma N_a \frac{\sigma_{\rm ex}}{\sigma_b}. \tag{A2}$$

Here N_γ is the number of photons within the tube with cross section σ_b and length $l = 100\,\text{km} = 10^7\,\text{cm} = 10^8\,\text{mm}$ during the time of the experiment, N_a is the same for the number of atoms, and $\sigma_{\rm ex}$ is the excitation cross section. For the rough estimate we accept for $\sigma_{\rm ex}$ the value $\sigma_{\rm ex} \approx 10^{-19}\,\text{cm}^2$ obtained with formula (38). With the number density for the atoms in the cavity $\rho_a = 10^{13}\,\text{cm}^{-3}$ we obtain $N_a = 10^{18}$. We accept that the typical intensity laser I can achieve is

$$I = N_\gamma \frac{\hbar\omega c}{V} = 10^{14}\ \text{Wt/cm}^2, \tag{A3}$$

where $\hbar\omega$ is the energy of one photon, c is the speed of the light, and V is the volume, in our case the volume of the long tube $V = 10^5\,\text{cm}^3$. For the valence electrons in heavy atoms, $\hbar\omega \approx 0.1$ a.u. $\approx 0.46\times10^{-11}$ erg. Then from Eq. (A3) it follows that $N_\gamma \approx 10^{27}$. For the total number of events according to Eq. (A2) it follows that $N_e \approx 10^{28}$ so that the inequality (A1) $N_e > 10^{18}$ is safely satisfied.

[1] J. H. Christenson, J. W. Cronin, V. L. Fitch, and R. Turlay, Phys. Rev. Lett. **13**, 138 (1964).
[2] E. M. Purcell and N. F. Ramsey, Phys. Rev. **78**, 807 (1950).
[3] E. E. Salpeter, Phys. Rev. **112**, 1642 (1958).
[4] P. G. H. Sandars, Phys. Lett. **14**, 194 (1965).
[5] V. V. Flambaum, Yad. Fiz. **24**, 383 (1976) [Sov. J. Nucl. Phys. **24**, 199 (1976)].
[6] P. G. H. Sandars, Phys. Rev. Lett. **19**, 1396 (1967).
[7] L. N. Labzovsky, Zh. Eksp. Teor. Fiz. **73**, 1623 (1977) [Sov. Phys. JETP **46**, 853 (1977)].
[8] L. N. Labzowsky, Zh. Eksp. Teor. Fiz. **75**, 856 (1978) [Sov. Phys. JETP **48**, 434 (1978)].
[9] O. P. Sushkov and V. V. Flambaum, Zh. Eksp. Teor. Fiz. **75**, 1208 (1978) [Sov. Phys. JETP **48**, 608 (1978)].
[10] V. G. Gorshkov, L. N. Labzowsky, and A. N. Moskalev, Zh. Eksp. Teor. Fiz. **76**, 414 (1979) [Sov. Phys. JETP **49**, 209 (1979)].
[11] A. A. Bondarevskaya, D. V. Chubukov, O. Yu. Andreev, E. A. Mistonova, L. N. Labzowsky, G. Plunien, D. Liesen, and F. Bosch, J. Phys. B **48**, 144007 (2015).
[12] B. C. Regan, E. D. Commins, C. J. Schmidt, and D. DeMille, Phys. Rev. Lett. **88**, 071805 (2002).
[13] J. J. Hudson, D. M. Kara, I. J. Smallman, B. E. Sauer, M. R. Tarbutt, and E. A. Hinds, Nature (London) **473**, 493 (2011).
[14] J. Baron *et al.* (ACME Collaboration), Science **343**, 269 (2014).
[15] W. B. Cairncross, D. N. Gresh, M. Grau, K. C. Cossel, T. S. Roussy, Y. Ni, Y. Zhou, J. Ye, and E. A. Cornell, Phys. Rev. Lett. **119**, 153001 (2017).
[16] A. V. Titov, N. S. Mosyagin, A. N. Petrov, T. A. Isaev, and D. DeMille, in *Recent Advances in the Theory of Chemical and Physical Systems*, edited by J.-P. Julien, J. Maruani, D. Mayou, S. Wilson, and G. Delgado-Barrio, Progress in Theoretical Chemistry and Physics Vol. 15 (Springer, Netherlands, 2006), Chap. 2, pp. 253–284.
[17] L. V. Skripnikov, J. Chem. Phys. **147**, 021101 (2017).
[18] T. Fleig, Phys. Rev. A **95**, 022504 (2017).
[19] F. Hoogeveen, Nucl. Phys. B **341**, 322 (1990).
[20] M. Pospelov and I. Khriplovich, Sov. Nucl. Phys. **53**, 638 (1991) [Yad. Fiz. **53**, 1030 (1991)].
[21] M. Pospelov and A. Ritz, Phys. Rev. D **89**, 056006 (2014).
[22] D. V. Chubukov and L. N. Labzowsky, Phys. Rev. A **93**, 062503 (2016).
[23] N. B. Baranova, Yu. V. Bogdanov, and B. Ya. Zel'dovich, Usp. Fiz. Nauk **123**, 349 (1977) [Sov. Phys. Usp. **20**, 1977 (1978)].
[24] L. M. Barkov, M. S. Zolotarev, and D. A. Melik-Pashaev, Pis'ma Zh. Eksp. Teor. Fiz. **48**, 134 (1988) [JETP Lett. **48**, 144 (1988)].
[25] D. F. Kimball, D. Budker, D. S. English, C.-H. Li, A.-T. Nguyen, S. M. Rochester, A. Sushkov, V. V. Yashchuk, and M. Zolotorev, in *Art and Symmetry in Experimental Physics*, edited by D. Budker, P. H. Bucksbaum, and S. J. Freedman, AIP Conf. Proc. No. 596 (AIP, New York, 2001), p. 84.
[26] D. Budker, W. Gawlik, D. Kimball, S. M. Rochester, V. Yashchuk, and A. Weis, Rev. Mod. Phys. **74**, 1153 (2002).
[27] L. Bougas, G. E. Katsoprinakis, W. von Klitzing, and T. P. Rakitzis, Phys. Rev. A **89**, 052127 (2014).
[28] V. M. Baev, T. Latz, and P. E. Toschek, Appl. Phys. B **69**, 171 (1999).
[29] M. Durand, J. Morville, and D. Romanini, Phys. Rev. A **82**, 031803 (2010).
[30] D. V. Chubukov and L. N. Labzowsky, Phys. Rev. A **96**, 052105 (2017).
[31] I. B. Khriplovich, *Parity Nonconservation in Atomic Phenomena* (Gordon and Breach, London, 1991).
[32] O. Yu. Andreev, L. N. Labzowsky, G. Plunien, and D. A. Solovyev, Phys. Rep. **455**, 135 (2008).
[33] V. N. Novikov, O. P. Sushkov, and I. B. Khriplovich, Opt. Spectrosk. **43**, 621 (1977) [transl. Opt. Spectrosc. (USSR) **43**, 370 (1977)].
[34] G. J. Roberts, P. E. G. Baird, M. W. S. M. Brimicombe, P. G. H. Sandars, D. R. Selby, and D. N. Stacey, J. Phys. B **13**, 1389 (1980).
[35] A. I. Akhiezer and V. B. Berestetskii, *Quantum Electrodynamics* (Wiley, New York, 1965).
[36] H. Bethe and E. Salpeter, *Quantum Mechanics of One- and Two-Electron Atoms* (Springer, New York, 1957).
[37] L. I. Schiff, Phys. Rev. **132**, 2194 (1963).
[38] E. Lindroth, B. W. Lynn, and P. G. H. Sandars, J. Phys. B **22**, 559 (1989).
[39] L. Bougas, G. E. Katsoprinakis, W. von Klitzing, J. Sapirstein, and T. P. Rakitzis, Phys. Rev. Lett. **108**, 210801 (2012).
[40] L. D. Landau and E. M. Lifshits, *Quantum Mechanics: Nonrelativistic Theory* (Pergamon Press, New York, 1977).
[41] I. I. Sobel'man, *Atomic Spectra and Radiative Transitions* (Springer, Berlin, 1979).

[42] L. V. Skripnikov, A. V. Titov, A. N. Petrov, N. S. Mosyagin, and O. P. Sushkov, Phys. Rev. A **84**, 022505 (2011).
[43] L. V. Skripnikov, D. E. Maison, and N. S. Mosyagin, Phys. Rev. A **95**, 022507 (2017).
[44] L. Visscher, E. Eliav, and U. Kaldor, J. Chem. Phys. **115**, 9720 (2001).
[45] K. G. Dyall, Theor. Chem. Acc. **117**, 491 (2007).
[46] K. G. Dyall, Theor. Chem. Acc. **131**, 1217 (2012).
[47] M. Kállay, J. Gauss, and P. G. Szalay, J. Chem. Phys. **119**, 2991 (2003).
[48] M. Kállay and J. Gauss, J. Chem. Phys. **121**, 9257 (2004).
[49] M. Kállay, P. G. Szalay, and P. R. Surján, J. Chem. Phys. **117**, 980 (2002).
[50] DIRAC, a relativistic ab initio electronic structure program, Release DIRAC12 (2012), written by H. J. Aa. Jensen, R. Bast, T. Saue, and L. Visscher, with contributions from V. Bakken, K. G. Dyall, S. Dubillard, U. Ekström, E. Eliav, T. Enevoldsen, T. Fleig, O. Fossgaard, A. S. P. Gomes, T. Helgaker, J. K. Lærdahl, Y. S. Lee, J. Henriksson, M. Iliaš, Ch. R. Jacob, S. Knecht, S. Komorovský, O. Kullie, C. V. Larsen, H. S. Nataraj, P. Norman, G. Olejniczak, J. Olsen, Y. C. Park, J. K. Pedersen, M. Pernpointner, K. Ruud, P. Sałek, B. Schimmelpfennig, J. Sikkema, A. J. Thorvaldsen, J. Thyssen, J. van Stralen, S. Villaume, O. Visser, T. Winther, and S. Yamamoto (see http://www.diracprogram.org).
[51] MRCC, a quantum chemical program suite written by M. Kállay, Z. Rolik, I. Ladjánszki, L. Szegedy, B. Ladóczki, J. Csontos, and B. Kornis. See also Z. Rolik and M. Kállay, J. Chem. Phys. **135**, 104111 (2011), as well as: www.mrcc.hu.
[52] L. V. Skripnikov, J. Chem. Phys. **145**, 214301 (2016).
[53] A. N. Petrov, L. V. Skripnikov, and A. V. Titov, Phys. Rev. A **96**, 022508 (2017).
[54] Z. W. Liu and H. P. Kelly, Phys. Rev. A **45**, R4210(R) (1992).
[55] V. A. Dzuba and V. V. Flambaum, Phys. Rev. A **80**, 062509 (2009).
[56] S. G. Porsev, M. S. Safronova, and M. G. Kozlov, Phys. Rev. Lett. **108**, 173001 (2012).
[57] Yu. M. Efremov, L. V. Gurwich, A. N. Savchenko, and E. A. Sviridenkov, Chem. Phys. Lett. **61**, 179 (1979).